1,4-dioxane degradation using a pulsed switching peroxi-coagulation process

Yaobin Lu, Hualei Shi, Jialiang Yao, Guangli Liu, Haiping Luo and Renduo Zhang

ABSTRACT

Widely used in chemical product manufacture, 1,4-dioxane is one of the emerging contaminants, and it poses great risk to human health and the ecosystem. The aim of this study was to degrade 1,4-dioxiane using a pulsed switching peroxi-coagulation (PSPC) process. The electrosynthesis of H_2O_2 on cathode and Fe^{2+} production on iron sacrifice anode were optimized to enhance the 1,4-dioxane degradation. Under current densities of 5 mA/cm^2 (H_2O_2) and 1 mA/cm^2 (Fe^{2+}), 95.3 ± 2.2% of 200 mg/L 1,4-dioxane was removed at the end of 120 min operation with the optimal pulsed switching frequency of 1.43 Hz and pH of 5.0. The low residual H_2O_2 and Fe^{2+} concentrations were attributed to the high pulsed switching frequency in the PSPC process, resulting in effectively inhibiting the side reaction during the ·OH production and improving the 1,4-dioxane removal with low energy consumption. At 120 min, the minimum energy consumption in the PSPC process was less than 20% of that in the conventional electro-Fenton process (7.8 ± 0.1 vs. 47.0 ± 0.6 kWh/kg). The PSPC should be a promising alternative for enhancing 1,4-dioxane removal in the real wastewater treatment.

Key words | 1,4-dioxane degradation, electro-Fenton, pulsed switching circuit, sacrifice iron anode

HIGHLIGHTS

- 1,4-dioxiane was efficiently removed in the PSPC process.
- Residual H_2O_2 and Fe^{2+} were minimized by optimizing pulsed switching circuits.
- The energy consumption in the PSPC reduced to 20% of that in the EF.

GRAPHICAL ABSTRACT

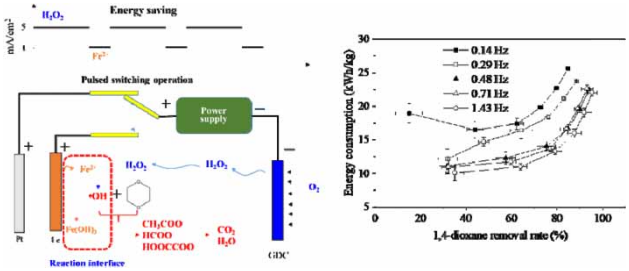

Yaobin Lu
Guangdong Provincial Key Laboratory of Water Quality Improvement and Ecological Restoration for Watersheds, Institute of Environmental and Ecological Engineering,
Guangdong University of Technology,
Guangzhou 510006,
China

Yaobin Lu
Hualei Shi
Guangli Liu (corresponding author)
Haiping Luo
Renduo Zhang
Guangdong Provincial Key Laboratory of Environmental Pollution Control and Remediation Technology, School of Environmental Science and Engineering,
Sun Yat-sen University,
Guangzhou 510006,
China
E-mail: *liugl@mail.sysu.edu.cn*

Jialiang Yao
The Affiliated High School of South China Normal University,
Guangzhou 510630,
China

doi: 10.2166/wrd.2021.092

INTRODUCTION

As an important solvent stabilizer, reaction agent, and reaction media, 1,4-dioxane ($C_4H_8O_2$) has been widely used in the manufacturing processes of chemical products such as paints, varnishes, lacquers, cosmetics, resins, and deodorants (Clercq *et al.* 2010; Barndõk *et al.* 2016a). Being possibly carcinogenic to humans and chemically stable, 1,4-dioxane can pose a great risk to human health and the ecosystem (Clercq *et al.* 2010; Takeuchi & Tanaka 2020; Zhao *et al.* 2020). Since 1,4-dioxane is bio-refractory, indicated by the low ratio of biochemical oxygen demand (BOD) to chemical oxygen demand (COD) (i.e. 0.06), non-volatility, and its miscibility with water (Nakagawa *et al.* 2016; Radcliffe & Page 2020; Rossum 2020; Somda *et al.* 2020), it is difficult to effectively remove it in typical biological wastewater treatments (Mahendra *et al.* 2013; Huang *et al.* 2018; Xu *et al.* 2020). For example, complete decomposition of 100 mg/L 1,4-dioxane in the activated sludge processes required 7 days (Sei *et al.* 2010). Even with pure culture, more than 25 h was needed for the 1,4-dioxane removal (Sun *et al.* 2010; Sei *et al.* 2013). The biological co-metabolism can be used to enhance the 1,4-dioxane degradation. However, additional nutrients, such as tetrahydrofuran and lactate (Sekar & DiChristina 2014), may increase the treatment cost (Hand *et al.* 2015; Zhang *et al.* 2016; Chen *et al.* 2020; Fan *et al.* 2020; Lin *et al.* 2020). Thus, it is necessary to develop an efficient method for 1,4-dioxane degradation.

The advanced oxidation processes (AOPs) have been developed for 1,4-dioxane removal in recent years. Compared with the biological treatment process, AOPs can produce high reactive and non-selective oxidant (i.e. ·OH) (Elkacmi & Bennajah 2019), and thus are a fast and efficient alternative to 1,4-dioxane degradation (Clercq *et al.* 2010; Barndõk *et al.* 2016a). Because of its good performance, easy control, and environmental friendliness (Wang *et al.* 2016), the Fenton process is one of the powerful AOPs for 1,4-dioxane removal. The Fenton process could reduce 1,4-dioxane from 100 to 0.5 mg/L within 6 h (Nakagawa *et al.* 2016). However, the high risk of H_2O_2 transport limits application of the Fenton process (Brillas & Martínez-Huitle 2015; Gao *et al.* 2015; Wang *et al.* 2016). The risks of H_2O_2 transport can be avoided by in-situ H_2O_2 production using the electro-Fenton (EF) process (Brillas & Martínez-Huitle 2015). As a combined EF process, the peroxi-coagulation (PC) process utilizes a sacrificial iron anode and a gas diffusion cathode (GDC) for H_2O_2 generation (Brillas *et al.* 2009). Fe^{2+} ions can release from the sacrificial iron anode to catalyze H_2O_2 for hydroxyl radicals (·OH) production. Excess Fe^{2+} dissolution from the iron anode can form $Fe(OH)_3$ precipitation as a coagulant. However, excess Fe^{2+} may also result in severe OH scavenger and high iron sludge production (Sun & Pignatello 1993; Benhadji *et al.* 2016).

Recently, a pulsed switching peroxi-coagulation (PSPC) process was developed for effectively controlling Fe^{2+} consumption (Lu *et al.* 2018). The controllable Fe^{2+} release in the auxiliary anode and H_2O_2 electrosynthesis in the cathode of PSPC was useful for maximum ·OH production and minimum iron sludge (Lu *et al.* 2018). Under current densities of 5.0 mA/cm^2 (H_2O_2) and 0.5 mA/cm^2 (Fe^{2+}), and the pulsed switching frequency of 1.0 s (H_2O_2): 0.3 s (Fe^{2+}), 500 mg/L 2,4-dichlorophenoxyacetic acid was completely removed in the PSPC within 240 min (Lu *et al.* 2018). The energy consumption for 500 mg/L 2,4-dichlorophenoxyacetic acid removal in the PSPC was only 50% of that in the conventional EF process (68 ± 6 vs. 136 ± 10 kWh/kg TOC) (Lu *et al.* 2018). The iron consumption in the PSPC was only ~5% of that in the conventional PC process. Although PSPC showed great potential in the 2,4-dichlorophenoxyacetic acid removal, the application of PSPC is still in its infancy and needs further testing for other refractory organics. Moreover, the physicochemical characteristics of different refractory organics can affect its removal in the AOPs (Clercq *et al.* 2010; Lu *et al.* 2018). For example, 1,4-dioxane has higher solubility and toxicity than 2,4-dichlorophenoxyacetic acid (Clercq *et al.* 2010; Lu *et al.* 2018). The optimal operational conditions for 1,4-dioxane removal in the PSPC may be different from those for 2,4-dichlorophenoxyacetic acid removal. The experiments on 1,4-dioxane removal in the PSPC should be not only important for enhancing 1,4-dioxane degradation in the wastewater treatment but also for expanding the potential application of PSPC. Thus, the objective of this study was to investigate the

feasibility of the PSPC process for 1,4-dioxane degradation. The effect of H_2O_2 and Fe^{2+} production, pulsed switching frequency and current density were tested on the 1,4-dioxane removal. Five control experiments were carried out to distinguish the PSPC process from the EF and PC processes. The main intermediates of 1,4-dioxane degradation and the residual Fe^{2+} and H_2O_2 were identified to discuss the mechanism of efficient 1,4-dioxane degradation in the PSPC process.

MATERIALS AND METHODS

PSPC setup

The PSPC process was investigated in an undivided electrochemical cell with a cylindrical chamber (diameter × length = 3 × 4.5 cm). A platinum wire electrode (CHI115, CH Instrument, Inc., Shanghai, China) and an iron mesh (diameter of 3 cm, thickness of 0.3 mm, 90 meshes) were used as main and auxiliary anodes, respectively. A gas diffusion cathode (GDC) was constructed with a conductive gas diffusion layer, a catalyst layer, and a supporting layer of stainless steel mesh (90 meshes) (Wang *et al.* 2017). Carbon black powder (EC-300 J, Hesen, Shanghai, China) was used as a catalyst for H_2O_2 production. The effective surface area of the GDC was 7 cm^2. The distance between the GDC and Pt anode was 3.5 cm. The distance between the GDC and Pt anode was 2 cm. In-situ H_2O_2 and Fe^{2+} production was driven by the power supply (IT6700, ITECH Electronic Co., Ltd, Nanjing, China) with constant current. Two time relays with an accuracy of 0.1 s (ZYS48-S, Zhuoyi Electronic Co., Ltd, Shanghai, China) were used to control the pulsed switching circuits and the running time of H_2O_2 and Fe^{2+} productions in PSPC. A solution of 0.1 M Na_2SO_4 and 200 mg/L 1,4-dioxane (99%, Merck) was used as the electrolyte. The pH of the electrolyte was adjusted to 5.0 with H_2SO_4 or NaOH. The electrolyte was recycled in the electrochemical cell using a peristaltic pump (BT-100, Qite, China) with a flow rate of 36 mL/min.

Experimental procedure

The current density for H_2O_2 was set at 5.0 mA/cm^2 to produce H_2O_2 efficiently with low energy consumption based on the results of our preliminary tests. In order to avoid excess iron oxidization into Fe^{3+}, the current density for Fe^{2+} production was controlled at 1 mA/cm^2. The molar concentration ratio of Fe^{2+} to total Fe in the solution was >95% under the iron anode operation with 1 mA/cm^2. Thus, the pulsed switching ratio of H_2O_2 and Fe^{2+} productions were tested under the current densities of 5 mA/cm^2 for H_2O_2 and 1 mA/cm^2 for Fe^{2+}, including 4 s (H_2O_2): 4 s (Fe^{2+}) (i.e. 1.00), 4:3 s (i.e. 1.33), 4:2 s (i.e. 2.00), 4:1 s (i.e. 4.00), and 4:0.5 s (i.e. 8.00). The pulsed switching frequency, including 4:3 s (0.14 Hz), 2:1.5 s (0.29 Hz), 1.2:0.9 s (0.48 Hz), 0.8:0.6 s (0.71 Hz), and 0.4:0.3 s (1.43 Hz), was tested under the fixed pulsed switching ratio between H_2O_2 and Fe^{2+} productions of 1.33 (4/3 s), respectively. Under the pulsed switching frequency of 1.43 Hz, the 1,4-dioxane removal was tested under different current densities, including 15 mA/cm^2 (H_2O_2) +3 mA/cm^2 (Fe^{2+}), 10 mA/cm^2 (H_2O_2) +2 mA/cm^2 (Fe^{2+}), 5 mA/cm^2 (H_2O_2) +1 mA/cm^2 (Fe^{2+}), and 2.0 mA/cm^2 (H_2O_2) +0.4 mA/cm^2 (Fe^{2+}), respectively.

Five controls were used to distinguish the PSPC process from others, such as EF and PC processes (Brillas *et al.* 2009; Ahangarnokolaei *et al.* 2017). Control 0 was to test the 1,4-dioxane adsorption in the cell without H_2O_2 and Fe^{2+} production (Table 1). Control 1 was a conventional PC process to keep a continuous production of H_2O_2 and Fe^{2+} without the pulsed switching frequency in the cell under the current densities of 5 mA/cm^2 (H_2O_2) and 1 mA/cm^2 (Fe^{2+}). Control 2 was a conventional EF process to keep a continuous H_2O_2 production of 5 mA/cm^2, and add 7.9 mM Fe^{2+} into the cell without iron anode operation. Control 3 was to keep a pulsed H_2O_2 production at 5 mA/cm^2 with the pulsed switching frequency of 0.4:0.3 s (1.43 Hz), and 7.9 mM Fe^{2+} added into the cell without iron anode operation. Control 4 was to

Table 1 | Operational conditions in five controls

Control experiment	Current density for H_2O_2 production (mA/cm^2)	Current density for Fe^{2+} production (mA/cm^2)
Control 0	0	0
Control 1	5	1
Control 2	5	0[b]
Control 3	5[a]	0[b]
Control 4	5	0

[a]Pulsed H_2O_2 production at 5 mA/cm^2 and the pulsed switching frequency of 0.4:0.3 s (1.43 Hz).
[b]7.9 mM Fe^{2+} addition into cell without iron anode operation.

keep a continuous H_2O_2 production of 5 mA/cm^2, and add 7.9 mM Fe^{2+} into the cell without iron anode operation. The addition of 7.9 mM Fe^{2+} was equal to the total Fe^{2+} production in the PSPC process under the pulsed switching frequency ratio of 0.4:0.3 s, and current densities of 5 mA/cm^2 (H_2O_2) and 1 mA/cm^2 (Fe^{2+}) within 120 min.

Analysis and calculation

The H_2O_2 concentration was measured using a spectrophotometer (T6, Persee, Beijing, China) according to the titanium (IV) sulfate method (Barazesh *et al.* 2015). Fe^{2+} and total iron concentrations were determined with the phenanthroline spectrophotometric method (Xu *et al.* 2013). The total organic carbon (TOC) was measured using a Shimadzu TOC-L CPH analyzer (Shimadzu Co., Japan). The pH was measured by a pH meter (FE20, Mettler-Toledo, Switzerland). The total COD (TCOD) and soluble COD (SCOD) was determined using the dichromate standard method according to the samples filtrated without or with a 0.22 μm filter, respectively (Liu *et al.* 2015; Ye *et al.* 2017). A high performance liquid chromatograph (HPLC, P230II, Dalian Yilite Analytic Instrument Co. Ltd, China) was used to determine 1,4-dioxane concentration. A 10:90 (v/v) acetonitrile/water (phosphate buffer of pH 3) solution at 1.0 mL/min was used as the mobile phase. The chromatograph was equipped with a SinoChrom ODS-BP column (5 μm, 4.6 mm × 25 cm, Dalian Yilite Analytic Instrument Co. Ltd, China). The UV detector was set at 190 nm and the temperature was maintained at 30°. The intermediates of 1,4-dioxane degradation, including oxalic, acetic and formic acids, were quantified by an ion chromatograph (IC, CIC-D100, SHINE IC Solution Experts, China).

The energy consumption in the PSPC process was calculated based on the electricity consumption for H_2O_2 and Fe^{2+} production, except for the energy for electrolyte recirculation in the cell. The energy input (P, W) and energy consumption per kg 1,4-dioxane removal (EC, kWh/kg) were calculated as follows:

$$P = U_1 I_1 a + U_2 I_2 b \quad (1)$$

$$EC = \frac{1000Pt}{V_s \Delta C} \quad (2)$$

where V_s is the solution volume (L); I_1 and I_2 are the currents for H_2O_2 and Fe^{2+} production, respectively (A); U_1 and U_2 are the voltages for H_2O_2 and Fe^{2+} production, respectively (V); a is the ratio between the running time for H_2O_2 production and the whole operation time (h); b is the ratio between the running time for Fe^{2+} production and the whole operation time (h); t is the operation time (h); and ΔC is the decrement of 1,4-dioxane concentration in the PSPC process during the experiment (mg/L). The current efficiency of H_2O_2 production was estimated as previously described (Luo *et al.* 2015).

RESULTS

Effect of the pulsed switching ratio of H_2O_2 and Fe^{2+} productions on 1,4-dioxane degradation

In the PSPC process, the molar ratio of H_2O_2 and Fe^{2+} concentrations were determined by the pulsed switching ratio of H_2O_2 and Fe^{2+} production. For example, when the pulsed switching ratio of H_2O_2 and Fe^{2+} production increased from 1.00 to 8.00, the molar ratio of H_2O_2 and Fe^{2+} increased from 1.49 to 12.0. As shown in Figure 1(a), more than 80% of 1,4-dioxane was removed under different pulsed switching ratios of H_2O_2 and Fe^{2+} production within 120 min. The 1,4-dioxane removal slightly increased from 80.1 ± 1.8 to 89.6 ± 1.1% with the pulsed switching ratio increasing from 1.00 to 8.00. The low pulsed switching ratio resulted in low energy consumption (Figure 1(b)). The energy consumption under the pulsed switching ratio of 1.33 was 25.6 kWh/kg, which was only 76% of that under the pulsed switching ratio of 8.00. The energy consumption was almost kept stable at the pulsed switching ratio of 1.33 and 1.00. Therefore, the pulsed switching ratio of 1.33 could be suitable for 1,4-dioxane removal in the PSPC process. Correspondingly, the molar ratio of H_2O_2 and Fe^{2+} was 1.99, and the 1,4-dioxane removal efficiency was 84 ± 2%.

Effect of pulsed switching frequency of H_2O_2 and Fe^{2+} production on 1,4-dioxane degradation

Under the fixed pulsed switching ratio of 1.33, different pulsed switching frequency, including 0.14, 0.29, 0.48,

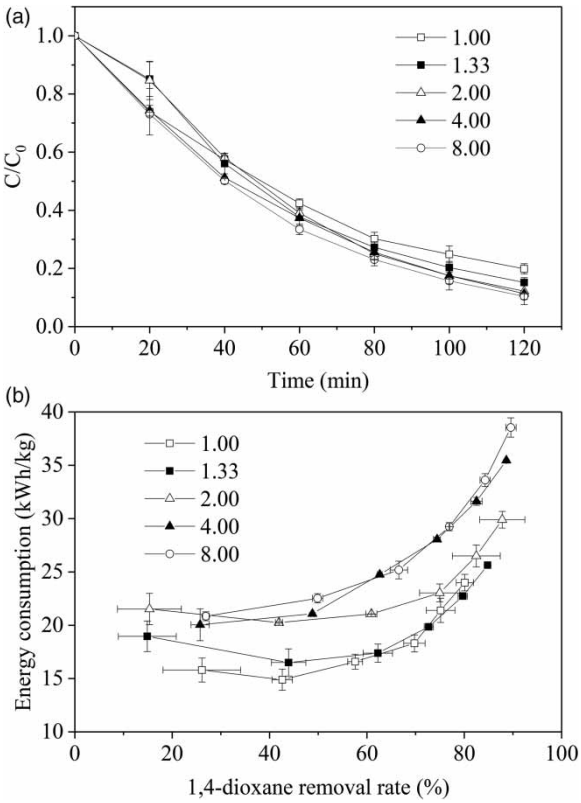

Figure 1 | (a) 1,4-dioxane removal and (b) energy consumption under different pulsed switching ratios of H_2O_2 and Fe^{2+} within 120 min (current densities of 5 mA/cm^2 for H_2O_2 production and 1 mA/cm^2 for Fe^{2+} production).

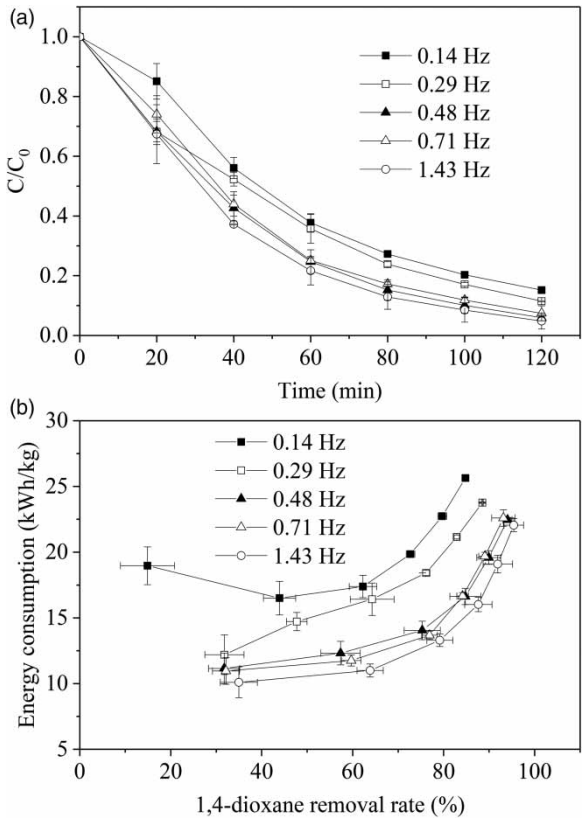

Figure 2 | Effect of pulsed switching frequency on (a) 1,4-dioxane removal and (b) energy consumption in the PSPC process (pulsed switching ratio of 1.33, current densities of 5 mA/cm^2 for H_2O_2 production and 1 mA/cm^2 for Fe^{2+} production).

0.71, and 1.43 Hz, was tested as shown in Figure 2. High pulsed switching frequency resulted in high 1,4-dioxane removal and low energy consumption. The 1,4-dioxane removal gradually increased from 84.8 ± 0.4 to 95.3 ± 2.2% with the pulsed switching frequency increasing from 0.14 to 1.43 Hz within 120 min. Based on Equation (1), the energy input for H_2O_2 and Fe^{2+} production was determined by the pulsed switching ratio of H_2O_2 and Fe^{2+} production. Under the pulsed switching ratio of 1.33, the energy input of the PSPC process was about 0.0718 W with 80% 1,4-dioxane removal, 96% of which was consumed by H_2O_2 generation. With the pulsed switching frequency increasing from 0.14 to 1.43 Hz, the energy consumption of the PSPC process with 80% 1,4-dioxane removal was decreased from 23 to 14 kWh/kg (Figure 2(b)). Therefore, the pulsed switching frequency of H_2O_2 and Fe^{2+} production was optimized to 0.4:0.3 s in the PSPC process. Correspondingly, 95.3 ± 2.2% of 1,4-dioxane was removed with the energy consumption of 22.1 ± 0.5 kWh/kg within 120 min.

Effect of current densities in the PSPC process on 1,4-dioxane degradation

Under the optimally pulsed switching frequency of 1.43 Hz, the effect of current densities in the PSPC process was tested as shown in Table 2. To keep the optimal molar ratio of H_2O_2 and Fe^{2+} production as described above, the current densities of H_2O_2 and Fe^{2+} production were changed proportionally, including 15 mA/cm^2 (H_2O_2) +3 mA/cm^2 (Fe^{2+}), 10 mA/cm^2 (H_2O_2) +2 mA/cm^2 (Fe^{2+}), 5 mA/cm^2 (H_2O_2) +1 mA/cm^2 (Fe^{2+}), and 2.0 mA/cm^2 (H_2O_2) +0.4 mA/cm^2 (Fe^{2+}). High current density of H_2O_2 and Fe^{2+} resulted in high 1,4-dioxane removal under the optimally pulsed switching frequency in the PSPC process (Table 2). However, even with low current densities such as 2.0 mA/cm^2 (H_2O_2) and 0.4 mA/cm^2 (Fe^{2+}), 89.8 ± 2.2% of 1,4-dioxane was still removed within 120 min.

Table 2 | The 1,4-dioxane removal in the PSPC processes and different controls

	1,4-Dioxane removal (%)								
	Current densities (mA/cm^2) in the PSPC process (pulsed switching frequency = 1.43 Hz)								
Time (min)	15 (H_2O_2) + 3 (Fe^{2+})	10 (H_2O_2) + 2 (Fe^{2+})	5 (H_2O_2) + 1 (Fe^{2+})	2.0 (H_2O_2) + 0.4 (Fe^{2+})	Control 0	Control 1	Control 2	Control 3	Control 4
20	52.9 ± 1.7	50.4 ± 5.8	32.6 ± 9.9	28.2 ± 3.1	3.4 ± 3.1	33.0 ± 5.2	59.0 ± 0.2	57.3 ± 6.4	6.4 ± 3.8
40	78.7 ± 1.1	77.4 ± 4.7	62.8 ± 0.2	49.2 ± 6.5	4.8 ± 2.5	66.0 ± 3.6	65.0 ± 2.4	63.2 ± 1.5	11.3 ± 2.7
60	90.5 ± 1.7	88.7 ± 3.9	78.3 ± 4.8	64.2 ± 3.3	6.9 ± 3.3	82.4 ± 3.3	66.6 ± 2.1	65.4 ± 2.0	13.9 ± 3.9
80	95.2 ± 1.4	94.1 ± 3.1	87.1 ± 4.2	77.4 ± 5.4	10.2 ± 1.4	92.0 ± 2.7	68.8 ± 2.2	67.9 ± 1.2	18.0 ± 3.1
100	98.2 ± 0.1	96.6 ± 2.3	91.5 ± 4.0	83.9 ± 1.4	10.7 ± 1.4	96.5 ± 1.7	70.9 ± 1.7	69.8 ± 0.8	18.6 ± 2.3
120	98.8 ± 0.5	97.7 ± 1.7	95.3 ± 2.2	89.8 ± 2.2	11.3 ± 2.2	97.2 ± 2.0	74.2 ± 0.5	71.7 ± 0.4	19.0 ± 1.7

In terms of 1,4-dioxane removal within 120 min, the different processes were in the order as follows: PSPC ≈ Control 1 > Control 2 > Control 3≫Control 4 ≈ Control 0. Control 0 showed that the adsorption was not significant for 1,4-dioxane removal in the PSPC process. Without Fe^{2+} catalyst addition, 1,4-dioxane could be hardly removed by H_2O_2 oxidation (see Control 4). Control 1 (i.e. the conventional PC process) removed 1,4-dioxane efficiently but consumed ~18.2 mM Fe^{2+} from the iron electrode within 120 min. Control 2 (i.e. the EF process) removed less 1,4-dioxane than PC and PSPC processes. Control 3 showed that only pulsed H_2O_2 production with 7.9 mM Fe^{2+} addition did not remove 1,4-dioxane as efficiently as that in the PSPC process within 120 min (71.7 ± 0.4% vs. 95.3 ± 2.2%).

High current densities of H_2O_2 and Fe^{2+} production resulted in high energy consumption in the PSPC process (Table 3). The energy consumption under 15 mA/cm^2 (H_2O_2) +3 mA/cm^2 (Fe^{2+}) was 15 times higher than that under 2.0 mA/cm^2 (H_2O_2) +0.4 mA/cm^2 (Fe^{2+}) within 120 min (121.0 ± 0.6 vs. 7.8 ± 0.1 kWh/kg). Nevertheless, the minimum energy consumption in the PSPC process under 2.0 mA/cm^2 (H_2O_2) +0.4 mA/cm^2 (Fe^{2+}) was less than 20% of that in Control 1 and 2 within 120 min, respectively (Table 3).

Residual Fe^{2+} and H_2O_2 concentrations during 1,4-dioxane degradation in the PSPC process

Under the pulsed switching frequency of 1.43 Hz and current densities of 5 mA/cm^2 (H_2O_2) and 1 mA/cm^2 (Fe^{2+}), the residual Fe^{2+} and H_2O_2 concentrations during 1,4-dioxane degradation was determined in the PSPC process within

Table 3 | Energy consumption in the PSPC processes and different controls

	Energy consumption (kWh/kg)						
	Current density (mA/cm^2) in the PSPC process (pulsed switching frequency = 1.43 Hz)						
Time (min)	15 (H_2O_2) + 3 (Fe^{2+})	10 (H_2O_2) + 2 (Fe^{2+})	5 (H_2O_2) + 1 (Fe^{2+})	2.0 (H_2O_2) + 0.4 (Fe^{2+})	Control 1	Control 2	Control 3
20	36.7 ± 1.2	20.4 ± 1.8	10.1 ± 1.2	4.5 ± 0.5	21.9 ± 2.9	9.8 ± 0.0	5.8 ± 0.6
40	49.0 ± 0.7	26.6 ± 0.8	11.0 ± 0.5	5.0 ± 0.6	21.6 ± 1.3	17.9 ± 0.5	10.4 ± 0.2
60	64.2 ± 1.2	34.8 ± 0.5	13.3 ± 0.5	5.6 ± 0.2	25.7 ± 1.2	26.2 ± 0.7	15.1 ± 0.4
80	81.9 ± 1.2	44.2 ± 0.2	16.0 ± 0.5	6.1 ± 0.4	30.4 ± 0.8	33.8 ± 0.9	19.3 ± 0.3
100	101.0 ± 0.0	52.5 ± 0.3	19.1 ± 0.7	7.0 ± 0.1	36.5 ± 0.8	41.0 ± 0.7	23.5 ± 0.2
120	121.0 ± 0.6	62.9 ± 0.8	22.1 ± 0.5	7.8 ± 0.1	43.5 ± 1.1	47.0 ± 0.6	27.5 ± 0.3

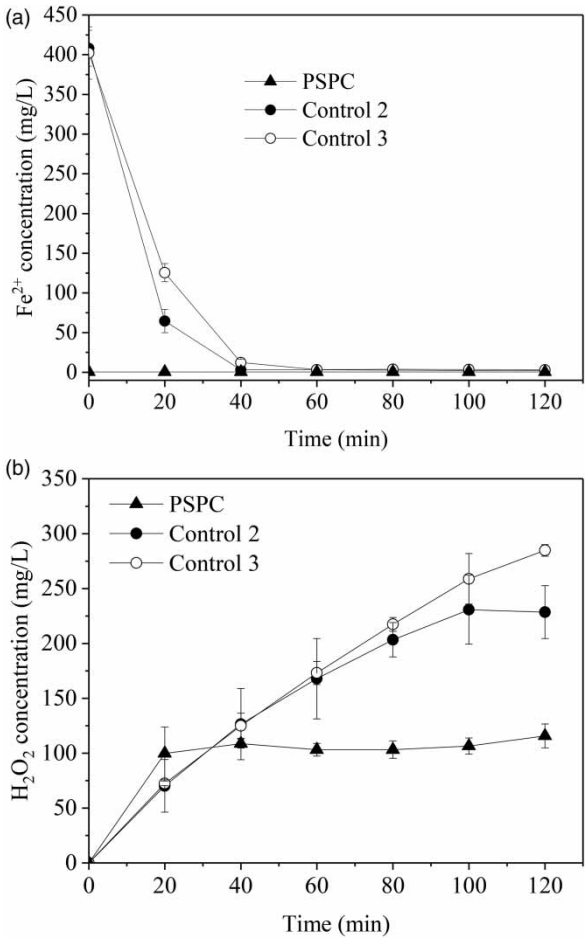

Figure 3 | Residual (a) Fe^{2+} and (b) H_2O_2 concentrations in PSPC process (pulsed switching frequency of 1.43 Hz, current densities of 5 mA/cm^2 for H_2O_2 production and 1 mA/cm^2 for Fe^{2+} production) and controls within 120 min.

120 min (Figure 3). The residual Fe^{2+} concentration was kept as low as 0.6 ± 0.5 mg/L within 120 min. The H_2O_2 concentration reached 100 mg/L and remained stable at 100 mg/L within 120 min. The residual Fe^{2+} and H_2O_2 concentrations in the PSPC process were different from that in Controls 2 and 3. With initial 7.9 mM Fe^{2+} addition, the residual Fe^{2+} concentration was decreased to <0.5 mg/L within 40 min in Controls 1 and 2. However, the residual H_2O_2 concentration was gradually increased to 280 and 250 mg/L in Controls 1 and 2, respectively. High residual Fe^{2+} concentration within 40 min and high residual H_2O_2 concentration within 40–120 min in Controls 1 and 2 may account for the lower 1,4-dioxane removal compared with that in the PSPC process. The residually soluble Fe^{3+} was not detected in all the tests, indicating that $Fe(OH)_3$ precipitated in the cell (Brillas *et al.* 2009).

Intermediates in the 1,4-dioxane degradation

Under the pulsed switching frequency of 1.43 Hz and current densities of 5 mA/cm^2 (H_2O_2) and 1 mA/cm^2 (Fe^{2+}), TCOD and SCOD in the cell were measured within 120 min as shown in Figure 4. The TCOD and SCOD concentrations decreased from 356 ± 28 to 119 ± 27 mg/L and from 356 ± 24 to 99 ± 10 mg/L within 120 min, respectively. Almost the same removals of TCOD and SCOD (67 vs. 72%) indicated that hydroxyl radical oxidation played the key role in the removal of 1,4-dioxane and its intermediates. Only 26.0% of TOC was removed in the PSPC system within 120 min, indicating that 1,4-dioxane was incompletely mineralized. High concentrations of the residual intermediates (e.g. small molecular organic acids) should account for low TOC removal in the 1,4-dioxane degradation in the PSPC process according to previous reports (Barndõk *et al.* 2016a). Acetic acid, formic acid, and oxalic acid were identified in the PSPC process (Figure 5). Under the pulsed switching frequency of 1.43 Hz and current densities of 5 mA/cm^2 (H_2O_2) and 1 mA/cm^2 (Fe^{2+}), the maximum formic acid concentration of 51.2 ± 0.3 mg/L was determined within 80 min. The concentrations of acetic acid, formic acid and oxalic acid were 10.0 ± 4.6, 31.1 ± 9.1, and 2.7 ± 0.8 mg/L at 120 min, respectively.

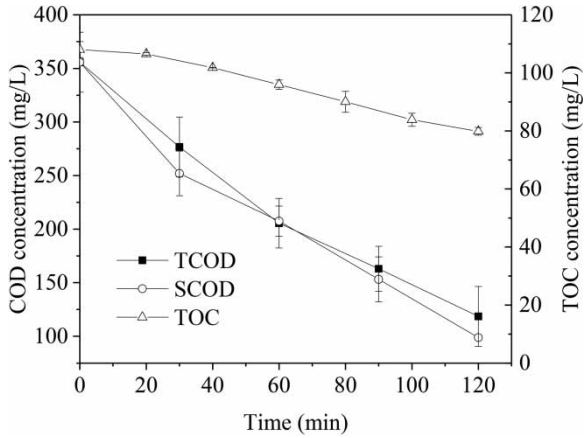

Figure 4 | Removal of TCOD, SCOD and TOC in the PSPC process within 120 min (pulsed switching frequency of 1.43 Hz, current densities of 5 mA/cm^2 for H_2O_2 production and 1 mA/cm^2 for Fe^{2+} production).

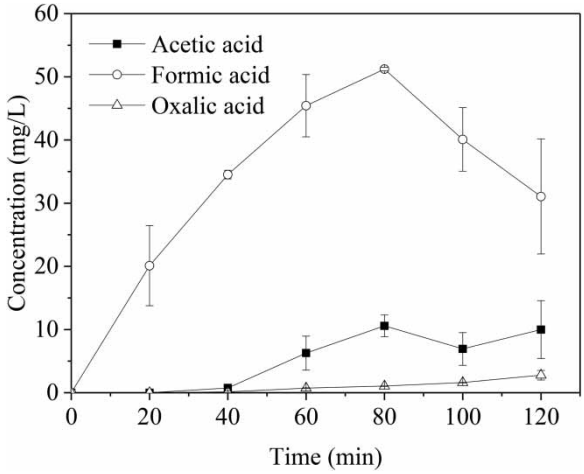

Figure 5 | Intermediate concentrations in the 1,4-dioxane degradation in the PSPC process (pulsed switching frequency of 1.43 Hz, current densities of 5 mA/cm^2 for H_2O_2 production and 1 mA/cm^2 for Fe^{2+} production).

DISCUSSION

During the hydroxyl radical production, many secondary reactions can occur in the Fenton process as follows:

$$Fe^{2+} + H_2O_2 + H^+ \rightarrow Fe^{3+} + H_2O + \cdot OH \quad K = 63M^{-1}\cdot s^{-1} \tag{3}$$

$$H_2O_2 + \cdot OH \rightarrow H_2O + HO_2\cdot \quad k_2 = 2.7\times10^7 M^{-1}\cdot s^{-1} \tag{4}$$

$$Fe^{2+} + \cdot OH \rightarrow Fe^{3+} + OH^- \quad k_2 = 3.2\times10^8 M^{-1}\cdot s^{-1} \tag{5}$$

$$Fe^{2+} + HO_2\cdot + H^+ \rightarrow Fe^{3+} + H_2O_2 \quad k_2 = 1.2\times10^6 M^{-1}\cdot s^{-1} \tag{6}$$

$$HO_2\cdot + HO_2\cdot \rightarrow H_2O_2 + O_2 \quad k_2 = 8.3\times10^5 M^{-1}\cdot s^{-1} \tag{7}$$

$$Fe^{3+} + H_2O_2 \rightarrow Fe^{2+} + HO_2\cdot + H^+ \quad k_2 = 0.01 M^{-1}\cdot s^{-1} \tag{8}$$

The excess of Fe^{2+} or H_2O_2 may give rise to the side reactions (4), (5), (6), and (7). As previously reported, the ·OH attacks the organics to form hydroxylated derivatives with a reaction rate (k_2) of about 10^7–10^9 M^{-1} s^{-1} (Brillas & Martínez-Huitle 2015; Gao *et al.* 2015), which is comparable to that in the side reactions (4), (5), (6), and (7). The reaction rate of 63 $M^{-1}\cdot s^{-1}$ in the ·OH production (Equation (3)) was much lower than those in Equations (4)–(7). Excess of Fe^{2+} or H_2O_2 can act as powerful competitors to the organics such as 1,4-dioxane to react with the ·OH (Sun & Pignatello 1993; Muruganandham & Swaminathan 2004). Therefore, excess of Fe^{2+} or H_2O_2 can result in low 1,4-dioxane removal and high energy consumption in the EF and PC processes. However, with the pulsed switching circuits, the excess of Fe^{2+} and H_2O_2 production was minimized in the PSPC process (Figure 3, Tables 1 and 2). The low residual Fe^{2+} concentration in the PSPC process within 120 min could be attributed to the high reduction activity of Fe^{2+} released from the iron sacrifice electrode, which can be rapidly consumed as described in Equation (3). However, low residual Fe^{2+} concentration in Controls 2 and 3 within 40–120 min indicated that not enough Fe^{2+} catalyzed H_2O_2 to produce ·OH. The Fe^{2+} in Controls 2 and 3 may be regenerated via the side reaction such as Equation (8) with low reaction rate, inhibiting efficient ·OH production. Therefore, the PSPC could have higher 1,4-dioxane removal with lower energy consumption compared with other processes.

The optimal molar ratio of H_2O_2 to Fe^{2+} (summarized as $[H_2O_2]/[Fe^{2+}]$) was greatly changed depending on the organics, solutions, etc. The optimal $[H_2O_2]/[Fe^{2+}]$ was in the range of 5–11 for the chlorinated aliphatic organic removal in the Fenton process (Tang & Huang 1997). $[H_2O_2]/[Fe^{2+}] = 1000{:}1$ had been reported to produce the highest ·OH concentration in the Fenton process among different molar ratios (Fischbacher *et al.* 2017). The theoretically optimal $[H_2O_2]/[Fe^{2+}]$ was 2.0 based on the pulsed switching ratio of 1.33 in this study, which was different from $[H_2O_2]/[Fe^{2+}] = 6$ for the 2,4-dichlorophenoxyacetic acid degradation in the PSPC process (Lu *et al.* 2018). It indicated that the pulsed switching ratio of H_2O_2 to Fe^{2+} should be further investigated to optimize $[H_2O_2]/[Fe^{2+}]$ during the PSPC application into the real wastewater treatment.

With a continuous consumption of H_2O_2 and Fe^{2+} as shown in Equation (3), lower H_2O_2 and Fe^{2+} concentrations were accumulated under higher pulsed switching frequency in the PSPC process. Similar results had been reported in the Fenton process with the stepwise addition of H_2O_2 to avoid excess H_2O_2 accumulation and decrease H_2O_2 scavenging ·OH (Zhang *et al.* 2012; Gan & Li 2013). With the pulsed switching frequency increasing from 0.71 to 1.43 Hz, the 1,4-dioxane removal was not significantly improved (93.1 ± 2.6 vs. 95.4 ± 2.2%), indicating the limited effect of high pulsed switching frequency on the 1,4-dioxane

removal. In addition, higher pulsed switching frequency will require higher precision of time relays and higher investment. Although the highest pulsed switching frequency of 1.43 Hz had the highest 1,4-dioxane removal with the lowest energy consumption in our PSPC process, the optimal pulsed switching frequency still needs further study in the PSPC process in future.

Because the residual H_2O_2 concentration was much higher than that of the residual Fe^{2+} concentration in the PSPC process, the ·OH production and 1,4-dioxane removal should occur close to the sacrifice iron electrode. However, with 7.9 mM Fe^{2+} addition in Control 2 (i.e. the EF process), the ·OH production and 1,4-dioxane removal could occur close to the cathode. Compared with the PSPC, the EF process may suffer from $Fe(OH)_3$ precipitation on the cathode surface, which can decrease the reaction area of H_2O_2 electro-generation in the cathode. Because of high solubility of 1,4-dioxane, the $Fe(OH)_3$ coagulation had no apparent effect on the 1,4-dioxane removal. The 1,4-dioxane degradation in the PSPC process was proposed as shown in Figure 6, based on the quantified intermediates. Various short chain organic acids have been identified in the intermediates of 1,4-dioxane degradation in AOPs (Barndõk *et al.* 2016a). In the UV photo-Fenton process, the intermediates such as acetic, oxalic, methoxyacetic and glycolic acids were identified during 7.3 g/L 1,4-dioxane degradation (Barndõk *et al.* 2016a). The maximum acetic acid concentration reached ~200 mg/L within 120 min (Barndõk *et al.* 2016a). In the solar photocatalysis using an NF-TiO_2 composite with TiO_2 nanoparticles, 140 mg/L 1,4-dioxane degradation resulted in the maximum formic acid of ~60 mg/L within 7 h (Barndõk *et al.* 2016b). Different AOPs including the PSPC showed that complete mineralization of 1,4-dioxane was greatly postponed due to high concentrations of short chain organic acids as intermediates (Barndõk *et al.* 2016a, 2016b). The short chain organic acids can be easily degraded by microbiology (Huang *et al.* 2017; Wu *et al.* 2020), thus the PSPC combined with a biological treatment process may be a potential way to mineralize 1,4-dioxane efficiently in future.

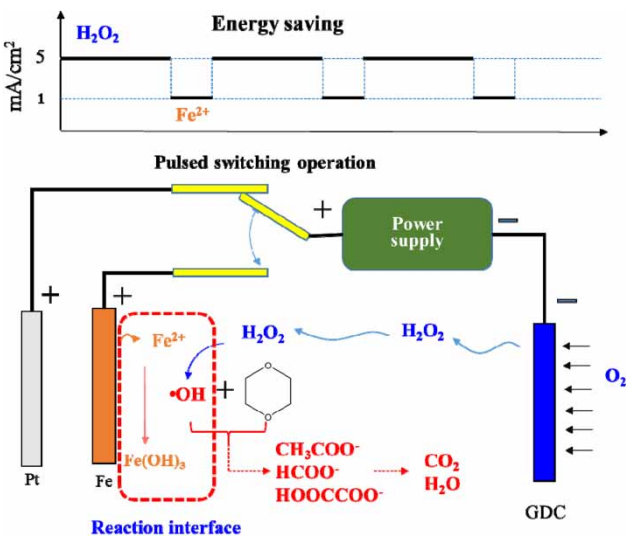

Figure 6 | Proposed degradation process of 1,4-dioxane in the PSPC.

CONCLUSIONS

The pulsed switching peroxi-coagulation (PSPC) process was used to remove 1,4-dioxane in this study. The pulsed switching ratio of H_2O_2 to Fe^{2+} production was optimized at 1.33. Under the optimized pulsed switching frequency of 1.43 Hz, the maximum 1,4-dioxane removal reached 98.8 ± 0.5% with the current densities of 15 mA/cm^2 (H_2O_2) +3 mA/cm^2 (Fe^{2+}) within 120 min. The minimum energy consumption reached 7.8 ± 0.1 kWh/kg with the current densities of 2.0 mA/cm^2 (H_2O_2) +0.4 mA/cm^2 (Fe^{2+}). At the end of 120 min operation, the residual Fe^{2+} concentration was kept as low as 0.6 ± 0.5 mg/L. Under the current densities of 5.0 mA/cm^2 (H_2O_2) +1 mA/cm^2 (Fe^{2+}), the residual H_2O_2 concentration reached 100 mg/L and remained stable at 100 mg/L. Low residual H_2O_2 and Fe^{2+} concentrations were attributed to high pulsed switching frequency in the PSPC process, resulting in effectively inhibiting the side reaction during the ·OH production and improving the 1,4-dioxane removal with low energy consumption. The quantified intermediates showed that the formic acid reached the maximum concentration of 51.2 ± 0.3 mg/L within 80 min. High concentrations of intermediates significantly hindered the mineralization of 1,4-dioxane.

ACKNOWLEDGEMENTS

This work was partly supported by grants from the Science and Technology Program of Guangzhou, China (No.

201804010450), the National Natural Science Foundation of China (Nos. 51608547, 51978676 and 51308557), the Guangdong Provincial Key Laboratory Project (2019B121203011), and the Fundamental Research Funds for the Central Universities (No. 19lgjc08).

DATA AVAILABILITY STATEMENT

All relevant data are included in the paper or its Supplementary Information.

REFERENCES

Ahangarnokolaei, M. A., Ganjidoust, H. & Ayati, B. 2017 Optimization of parameters of electrocoagulation/flotation process for removal of Acid Red 14 with mesh stainless steel electrodes. *Journal of Water Reuse and Desalination* **8** (2), 278–292.

Barazesh, J. M., Hennebel, T., Jasper, J. T. & Sedlak, D. L. 2015 Modular advanced oxidation process enabled by cathodic hydrogen peroxide production. *Environmental Science & Technology* **49** (12), 7391–7399.

Barndõk, H., Blanco, L., Hermosilla, D. & Blanco, Á. 2016a Heterogeneous photo-Fenton processes using zero valent iron microspheres for the treatment of wastewaters contaminated with 1,4-dioxane. *Chemical Engineering Journal* **284**, 112–121.

Barndõk, H., Hermosilla, D., Han, C., Dionysiou, D. D., Negro, C. & Blanco, Á. 2016b Degradation of 1,4-dioxane from industrial wastewater by solar photocatalysis using immobilized NF-TiO2 composite with monodisperse TiO2 nanoparticles. *Applied Catalysis B Environmental* **180**, 44–52.

Benhadji, A., Taleb Ahmed, M., Djelal, H. & Maachi, R. 2016 Electrochemical treatment of spent tan bath solution for reuse. *Journal of Water Reuse and Desalination* **8** (1), 123–134.

Brillas, E. & Martínez-Huitle, C. A. 2015 Decontamination of wastewaters containing synthetic organic dyes by electrochemical methods. An updated review. *Applied Catalysis B: Environmental* **166–167**, 603–643.

Brillas, E., Sirés, I. & Oturan, M. A. 2009 Electro-Fenton process and related electrochemical technologies based on Fenton's reaction chemistry. *Chemical Reviews* **109** (12), 6570–6631.

Chen, Z., Wu, G., Wu, Y., Wu, Q. & Hu, H. Y. 2020 Water Eco-Nexus Cycle System (WaterEcoNet) as a key solution for water shortage and water environment problems in urban areas. *Water Cycle* **1**, 71–77.

Clercq, J., Van de Steene, E., Verbeken, K. & Verhaege, M. 2010 Electrochemical oxidation of 1,4-dioxane at boron-doped diamond electrode. *Journal of Chemical Technology and Biotechnology* **85**, 1162–1167.

Elkacmi, R. & Bennajah, M. 2019 Advanced oxidation technologies for the treatment and detoxification of olive mill wastewater: a general review. *Journal of Water Reuse and Desalination* **9** (4), 463–505.

Fan, W., Yang, X., Wang, Y. & Huo, M. 2020 Loopholes in the current reclaimed water quality standards for clogging control during aquifer storage and recovery in China. *Water Cycle* **1**, 13–18.

Fischbacher, A., von Sonntag, C. & Schmidt, T. C. 2017 Hydroxyl radical yields in the Fenton process under various pH, ligand concentrations and hydrogen peroxide/Fe(II) ratios. *Chemosphere* **182**, 738–744.

Gan, P. P. & Li, S. F. Y. 2013 Efficient removal of Rhodamine B using a rice hull-based silica supported iron catalyst by Fenton-like process. *Chemical Engineering Journal* **229** (4), 351–363.

Gao, G., Zhang, Q., Hao, Z. & Vecitis, C. D. 2015 Carbon nanotube membrane stack for flow-through sequential regenerative electro-Fenton. *Environmental Science and Technology* **49** (4), 2375–2383.

Hand, S., Wang, B. & Chu, K. H. 2015 Biodegradation of 1,4-dioxane: effects of enzyme inducers and trichloroethylene. *Science of Total Environment* **520**, 154–159.

Huang, H., Chen, B.-Y. & Zhu, Z.-R. 2017 Formation and speciation of haloacetamides and haloacetonitriles for chlorination, chloramination, and chlorination followed by chloramination. *Chemosphere* **166**, 126–134.

Huang, H., Wu, J., Ye, J., Ye, T., Deng, J., Liang, Y. & Liu, W. 2018 Occurrence, removal, and environmental risks of pharmaceuticals in wastewater treatment plants in south China. *Frontiers of Environmental Science & Engineering* **12** (6), 69–79.

Lin, S., Xiao, L., Hu, Z. & Zhan, X. 2020 Nutrient recovery from animal manure using bipolar membrane electrodialysis: study on product purity and energy efficiency. *Water Cycle* **1**, 54–62.

Liu, G., Zhou, Y., Luo, H., Cheng, X., Zhang, R. & Teng, W. 2015 A comparative evaluation of different types of microbial electrolysis desalination cells for malic acid production. *Bioresoure Technology* **198**, 87–93.

Lu, Y., He, S., Wang, D., Luo, S., Liu, A., Luo, H., Liu, G. & Zhang, R. 2018 A pulsed switching peroxi-coagulation process to control hydroxyl radical production and to enhance 2,4-Dichlorophenoxyacetic acid degradation. *Frontiers of Environmental Science & Engineering* **12** (5), 9.

Luo, H., Li, C., Wu, C. & Dong, X. 2015 In situ electrosynthesis of hydrogen peroxide with an improved gas diffusion cathode by rolling carbon black and PTFE. *RSC Advances* **5** (80), 65227–65235.

Mahendra, S., Grostern, A. & Alvarez-Cohen, L. 2013 The impact of chlorinated solvent co-contaminants on the

biodegradation kinetics of 1,4-dioxane. *Chemosphere* **91** (1), 88–92.

Muruganandham, M. & Swaminathan, M. 2004 Decolourisation of Reactive Orange 4 by Fenton and photo-Fenton oxidation technology. *Dyes & Pigments* **63** (3), 315–321.

Nakagawa, H., Takagi, S. & Maekawa, J. 2016 Fered-Fenton process for the degradation of 1,4-dioxane with an activated carbon electrode: a kinetic model including active radicals. *Chemical Engineering Journal* **296**, 398–405.

Radcliffe, J. C. & Page, D. 2020 Water reuse and recycling in Australia- history, current situation and future perspectives. *Water Cycle* **1**, 19–40.

Rossum, T. V. 2020 Water reuse and recycling in Canada-history, current situation and future perspectives. *Water Cycle* **1**, 98–103.

Sei, K., Kakinoki, T., Inoue, D., Soda, S., Fujita, M. & Ike, M. 2010 Evaluation of the biodegradation potential of 1,4-dioxane in river, soil and activated sludge samples. *Biodegradation* **21** (4), 585–591.

Sei, K., Miyagaki, K., Kakinoki, T., Fukugasako, K., Inoue, D. & Ike, M. 2013 Isolation and characterization of bacterial strains that have high ability to degrade 1,4-dioxane as a sole carbon and energy source. *Biodegradation* **24** (5), 665–674.

Sekar, R. & DiChristina, T. J. 2014 Microbially driven Fenton reaction for degradation of the widespread environmental contaminant 1,4-dioxane. *Environmental Science & Technology* **48** (21), 12858–128567.

Somda, W., Tischbein, B. & Bogardi, J. 2020 Water use inside inland valleys agro-systems in the Dano Basin, Burkina Faso. *Water Cycle* **1**, 88–97.

Sun, Y. & Pignatello, J. J. 1993 Photochemical reactions involved in the total mineralization of 2,4-D by iron(3+)/hydrogen peroxide/UV. *Environmental Science & Technology* **27** (2), 304–310.

Sun, B., Ko, K. & Ramsay, J. A. 2010 Biodegradation of 1,4-dioxane by a Flavobacterium. *Biodegradation* **22** (3), 651–659.

Takeuchi, H. & Tanaka, H. 2020 Water reuse and recycling in Japan – history, current situation, and future perspectives. *Water Cycle* **1**, 1–12.

Tang, W. Z. & Huang, C. P. 1997 Stochiometry of Fenton's reagent in the oxidation of chlorinated aliphatic organic pollutants. *Environmental Technology* **18** (1), 13–23.

Wang, N., Zheng, T., Zhang, G. & Wang, P. 2016 A review on Fenton-like processes for organic wastewater treatment. *Journal of Environmental Chemical Engineering* **4** (1), 762–787.

Wang, W., Lu, Y., Luo, H., Liu, G. & Zhang, R. 2017 Effect of an improved gas diffusion cathode on carbamazepine removal using the electro-Fenton process. *RSC Advances* **7** (41), 25627–25633.

Wu, G., Yin, Q., Fang, G. & Hu, Z. 2020 Slow growers possess a high pollutant removal potential through granule formation for wastewater treatment. *Water Cycle* **1**, 63–69.

Xu, H. Y., Shi, T. N., Wu, L. C. & Qi, S. Y. 2013 Discoloration of methyl orange in the presence of Schorl and HO: kinetics and mechanism. *Water Air & Soil Pollution* **224** (10), 1–11.

Xu, A., Wu, Y. H., Chen, Z., Wu, G. & Hu, H. Y. 2020 Towards the new era of wastewater treatment of China: development history, current status, and future directions. *Water Cycle* **1**, 80–87.

Ye, B., Luo, H., Lu, Y., Liu, G., Zhang, R. & Li, X. 2017 Improved performance of the microbial electrolysis desalination and chemical-production cell with enlarged anode and high applied voltages. *Bioresource Technology* **244** (Pt 1), 913–919.

Zhang, H., Wu, X. & Li, X. 2012 Oxidation and coagulation removal of COD from landfill leachate by Fered–Fenton process. *Chemical Engineering Journal* **210** (4), 188–194.

Zhang, S., Gedalanga, P. B. & Mahendra, S. 2016 Biodegradation kinetics of 1,4-dioxane in chlorinated solvent mixtures. *Environmental Science & Technology* **50** (17), 9599–9607.

Zhao, Y., Ji, B., Liu, R., Ren, B. & Wei, T. 2020 Constructed treatment wetland: Glance of development and future perspectives. *Water Cycle* **1**, 104–112.

First received 16 October 2020; accepted in revised form 25 November 2020. Available online 17 February 2021